The ISO 5167 Compliant Design Venturi – A Further Summary of Calibration Experience

Kegel, T. M.
Colorado Engineering Station, Inc.
54043 WCR 37, Nunn, CO 80648 USA
(970)897-2711 tkegel@ceesi.com

Abstract: This is the second paper describing a program to organize and analyze the results of a large number of venturi meters calibrated using compressed air. Part four of the ISO 5167 standard specifies discharge coefficient values. The calibration results are organized into four categories based on a qualitative judgment as to how well the calibration fits the ISO coefficients. The database contained 59 venturies when the first paper was published; the current summary is based on 76 calibrations.

Keyword: venturi, ISO 5167, Herschel venturi, classical venturi

1. Introduction

Most differential producing flowmeters fit into one of four categories. The first category represents proprietary designs that will always need calibration. The second category, the orifice meter, is typically used without calibration. The calibration process is replaced with a detailed mechanical inspection, accompanied by a set of tolerance specifications documented in the ISO 5167 standard. If the orifice meter meets the geometric tolerance, an equation is provided allowing for the measurement of flowrate within a specified uncertainty. The third category consists of flow nozzles of various designs featuring either a circular or elliptical arc inlet. Over the years data have been published in attempts to substitute geometric inspection for flow calibration. This category also includes venturi designs based on circular arc inlets, basically a nozzle with attached diffuser.

The fourth category consists of the "Herschel" or "classical" venturi described in ISO 5167. This is the second paper that documents the analysis of a large database of ISO 5167 compliant venturi calibrations with the objective of identifying the consistency of calibration results and the dependence on geometric parameters. Currently the data base contains data from 76 venturies calibrated using compressed air. Inlet diameters range from 1.0 to 76 cm and beta ratios range from 0.11 to 0.75.

2. Boundary Layer Transition

The previous paper[1] introduced the common boundary layer model. While this model is commonly applied to venturies with circular arc inlets[2] the basic principle are applicable to the ISO 5167 compliant design. The topic is reviewed in the current paper based on one two calibration curves included in the database. Figure 1 shows data of discharge coefficient (C_d) plotted against Reynolds number (Re). The data fall into three Reynolds number regions: In the low Re region (125,000-223,000) the C_d rises with Re, a curve fit of the data is shown as a solid line. In the high Re region (742,000-1,350,000) the change in C_d with Re is much less, a second curve fit characterizes the data over this range. In these regions the throat boundary layer thickness is assumed to be increasing with Reynolds number. The presence of a boundary layer reduces the effective throat area which reduces the flowrate and therefore C_d.

The middle Reynolds number region (223,000-742,000) is assumed to correspond to the boundary layer transition from laminar to turbulent. As the flowrate increases the transition progresses gradually. At Re=223,000 turbulence begins to develop at one radial position within the throat, perhaps resulting from a rougher spot on the venturi surface. Assume the flowrate increases. As the Reynolds number increases, the turbulence "spot" increases in size. In addition, turbulence may develop at a second radial position within the throat. As the Reynolds number increases the percentage of the boundary layer that is laminar gradually decreases. Eventually the flowrate increases until Re=742,000 and the boundary layer if fully turbulent. The transition behavior illustrated in Figure 1 is sometimes identified as a "transition hump".

Figure 2 shows a calibration curve that exhibits no transition hump. It is assumed that the transition from laminar to turbulent boundary layers takes place over a very narrow Re range. It is further assumed that the boundary layer thickness does not appreciably change at the transition.

The form of equation usually applied in conjunction with the boundary layer model is:

$$C_d = a + bRe^c \qquad \text{[Eq. 1]}$$

Where usually c = -0.5 for a laminar boundary layer and c = -0.2 for a turbulent boundary layer.

The ISO 5167 standard recommends use of a venturi based on pairs of C_d and Re values. For the present analysis a curve fit of the form of Equation 1 has been calculated. The coefficient values are: a = 1.01091, b = - 9.51469 and c = -0.5.

The ISO standard places limits on inlet diameter, beta ratio, Reynolds number and flowing pressure when a predicted C_d is applied. When a venturi is applied outside the limits, calibration is recommended.

3. Classification

In the previous paper the calibration curves were classified into four "Types". The "b" coefficient in Equation 1 can be interpreted to represents the slope relating C_d and the term Re^c; estimated numerical slope values represented selection criteria. Calibrations classified as "Type A" exhibited a relatively lower net positive slope with little or no hump corresponding to boundary layer transition. The "Type B" calibrations exhibit a larger net positive slope and larger transition hump. Calibrations of "Type C" exhibit a net negative slope and a significant transition hump. The "Type D" calibrations are those that don't fit other categories.

The current analysis has maintained the philosophy of classification but has done so based on slightly different criteria. The main classification decision is based on agreement with the basic shape of the ISO curve. The previous classification criteria did not consider such agreement. The presence or absence of a transition hump is no longer a strong a criteria. Generally more data are available at Reynolds numbers above transition than below. Agreement with the ISO curve at high Re is therefore more important than agreement at low Re.

Towards the end of the first paper, a graph of calibration data was re-created based on shifted C_d values. In the present analysis the C_d data for each venturi has been shifted to best fit the ISO equation. It is assumed that the shift represents a change in the throat area, the difference between an "as designed" and "as built" throat diameter. The data for the current study is based exclusively on as designed values, actual throat diameters were not measured. The relationship between a shift in C_d and a shift in throat diameter cannot be confirmed.

Twenty calibrations are classified as Type A, the data are shown in Figure 3. The data for each venturi is shown as a solid black line. The dashed gray lines define a statistical interval centered on the ISO curve, the interval width is ±1%. Most of the data fit within the interval, some data from three venturies fall outside the interval.

In Figure 4 the statistical interval has been subdivide into three regions based on Reynolds number (Re). The Re range from 90,000 to 600,000 represents the transition between laminar and turbulent boundary layers. The transition always results in an increased C_d, the interval is characterized by +2%, -1%. For Re greater than 2 million the interval width is ±0.3%, a large concentration of data fall within this statistical interval. For Re less than 2 million, excluding transition, the interval width is ±1%.

Twenty eight calibrations are classified as Type B, the data are shown in Figure 5. Two data points for one venturi are off the chart (C_d=0.90786, Re=121,591 and C_d=0.91165, Re=121,605). The dashed gray lines represent statistical intervals presented in a format similar to Figure 3. For Re greater than 2 million the interval width is ±0.6%, double the corresponding Type A value. For Re less than 2 million the interval width is ±2%, also double the corresponding Type A value. The increased interval widths are the result of larger amplitude random effects as well as larger deviations from the ISO equation.

The amplitude of transition humps are similar for Type A and B, both are mostly contained below an upper limit of 2%. While the amplitudes are similar, the transition Reynolds number ranges appear to be broader for the Type B venturies. Aside from the differences in statistical intervals, the behavior above Re=2 million is quite similar for Type A and B. All the calibration curves are converging to the same nominal C_d values as Reynolds number increases.

The behavior below Re=300,000 is much more consistent for Type A than B. In most applications the higher Reynolds number behavior is more important than lower Reynolds number. In the classification process several Type B venturies fit the ISO equation much better at high Re than low Re.

Fourteen calibrations are classified as Type C, the data are shown in Figure 6. The dashed gray lines represent a statistical interval of ±2% in width. When compared to Type B, the curves are less likely to match the basic shape or slope of the ISO equation. The curves are more likely to display multiple uncharacteristic inflections points. The transition humps are observed at lower Re and random effects appear larger in amplitude. Very little Type C data are available at low Re values.

Fourteen calibrations are classified as Type D, the data are shown in Figure 7. The dashed gray lines represent a statistical interval of ±2% in width. The Type C and D data very similar when compared to Type B. The major difference is that the characteristics observed in C are more dramatic in D. Both Figures contain fourteen curves the Type D data are spread out a bit more. The Type C graph shows a concentration of data well centered in the interval over the Re range of 200,000 to 4,000,000. A similar concentration is not observed in the Type D graph.

4. Summary

Some characteristics of the four curve types are summarized in Table 1. The calibrations were sorted without regards to equalizing the distribution. Regardless, the process resulted in a similar

number of curves in each Type; slightly less in C and D with more in B. It appears as if each Type contains adequate data from which to draw statistical conclusions.

The C_d values were shifted to best fit the ISO equation. The qualitative classification process was based solely on the shape of the C_d vs Re curve, the magnitude of the C_d shift was not a criteria. Referring to Table 1, the average shift seems to correlate with Type; a lower average shift is observed with Type A, more with B still more with C and D. The shift is consistently in the same direction which seems to indicate that the ISO equation consistently predicts higher values of C_d. If the C_d values are shifted due to difference in throat diameter, a random distribution of shifted value would be expected.

The inlet diameter is slightly less for A and B than C and D. Smaller meters would seem to better fit the ISO equation, a limitation stated in ISO 5167. The average beta ratio shows no change based on classification. The rangeability for A and B is slightly larger than C and D, no explanation is proposed to explain this observation.

Many of the data sets (50) exhibit boundary layer transition. A subset (12) did not include data at a low enough Re value to identify the transition. For the remaining data sets (38) the transition hump was identified by Re and C_d. In Figure 1, for example, the transition is estimated to be Re=260,676 and C_d=1.01353. From Table 1, the fewest curves (as a percentage of total) with transition humps are classified as Type A and the most as Type B.

Data of transition Re plotted against inlet diameter are contained in Figure 8. The correlation coefficient is 0.4183 which means that 41% of the variation in Reynolds number is correlated with inlet diameter. A relationship between a Reynolds number and diameter makes intuitive sense; the data seem to indicate such a relationship in the present data. The earlier discussion described the boundary layer development along the inlet surface. The boundary layer thickness is therefore a function of the length which will in turn depend on throat as well as inlet diameter. A plot of transition Reynolds number against development length resulted in a correlation coefficient value of 0.3759. Further, plotting transition Reynolds number against beta ratio shows no correlation. It appears the transition Reynolds number depends more on inlet diameter than throat diameter or beta ratio.

The "size" or amplitude of a transition hump is first recorded as the value of C_d and then expressed as a percentage shift from the ISO equation. In Table 1 the average transition hump amplitude clearly correlates with Type, the value steadily increases from A to B to C and D. As the transition hump amplitude increases, the venturi calibration is less likely to fit the ISO equation. Further investigation indicated no correlation when plotted against inlet diameter or beta ratio.

5. Conclusions

A large database of ISO 5167 compliant venturi calibrations is being investigated.

A Type A venturi will fit the ISO equation to within ±1% based on two assumptions. First, it is assumed that the transition from laminar to turbulent flow in the boundary layer results in a small change in C_d. Second, the throat diameter has been correctly measured. The second assumption has not been confirmed based on the current data because throat diameter measurements were not made. A Type B venturi will fit the ISO equation to within ±2% based on two assumptions.

A Type C or D venturi exhibits a calibration curve that differs significantly from the ISO equation. Calibration is recommended.

The ISO standard places limits on inlet diameter, beta ratio, Reynolds number and flowing pressure when a predicted C_d is applied. When a venturi is applied outside the limits, calibration is recommended. The present study did not evaluate the limits specified by the ISO standard.

It appears that the ISO predicts a C_d that is between 1% and 1.5% high.

A significant percentage (37%) of the venturi calibrations are classified as either C or D. Without direct calibration a venturi cannot be classified, it is recommended that all venturies be calibrated.

6. References

1. ISO 5167: Measurement of fluid flow by means of pressure differential devices inserted in circular cross-section conduits running full — Part 4: Venturi tubes, International Standards Organization, 2003.

2. Kegel, T. M., "The ISO 5167 Compliant Design Venturi – A Summary of Calibration Experience," International Symposium on Fluid Flow Measurement, 2009.

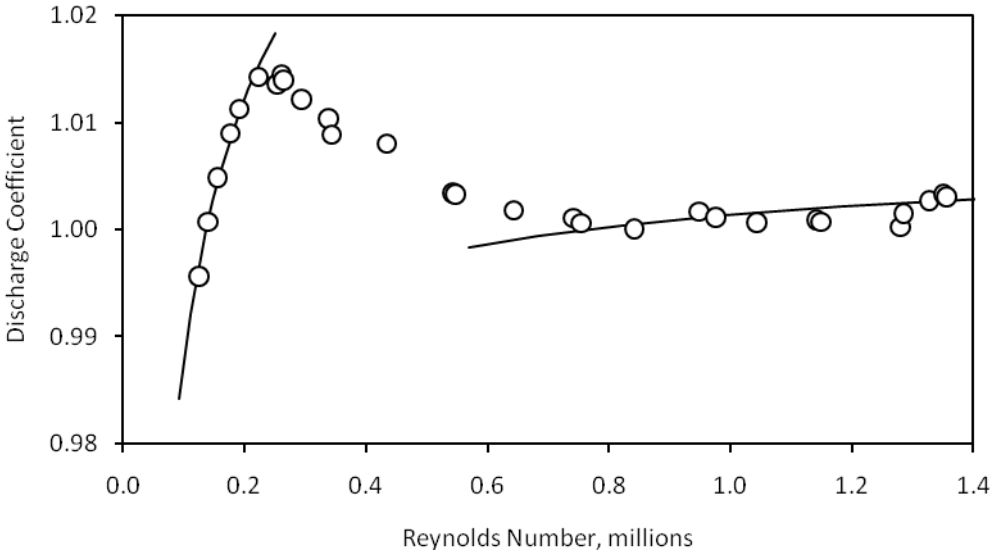

Figure 1: Calibration Results with a Large Transition Hump

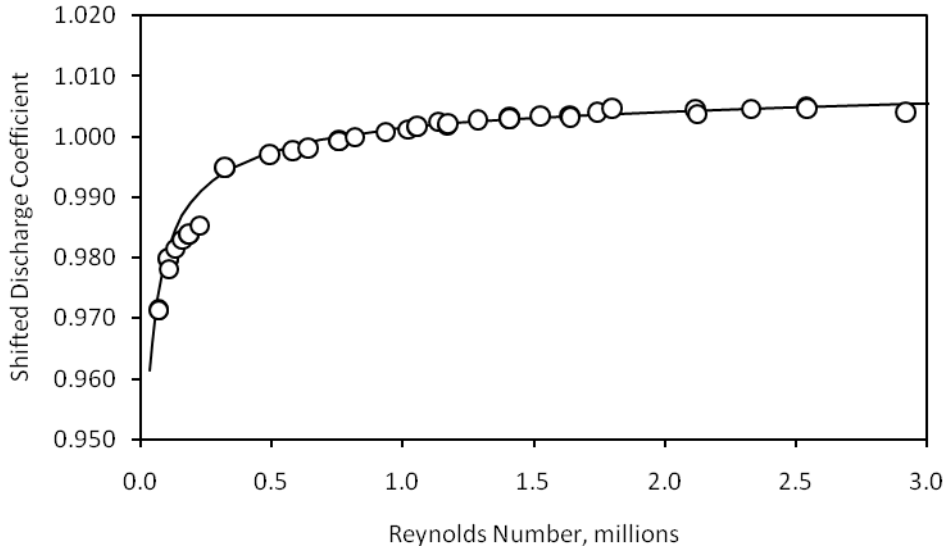

Figure 2: Calibration Results without a Large Transition Hump

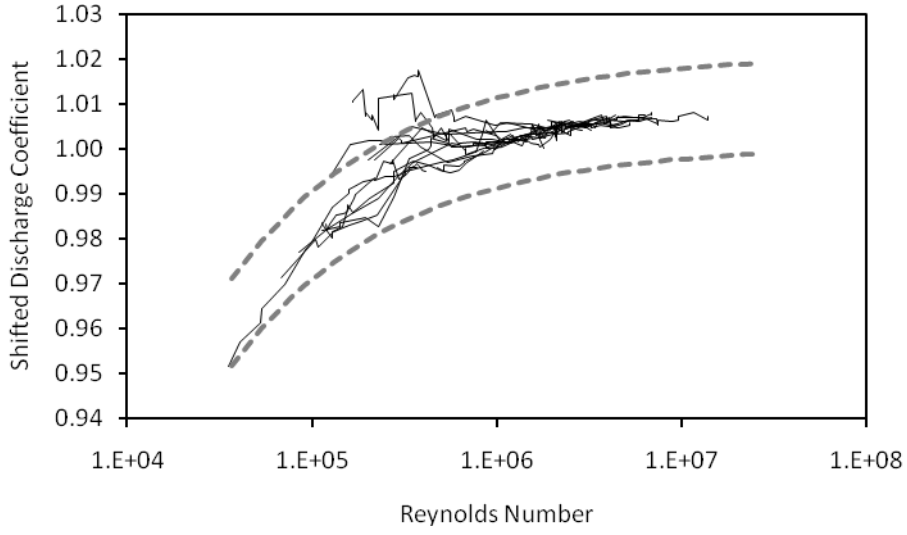

Figure 3: Calibrations Classified as Type A, Uniform Statistical Interval

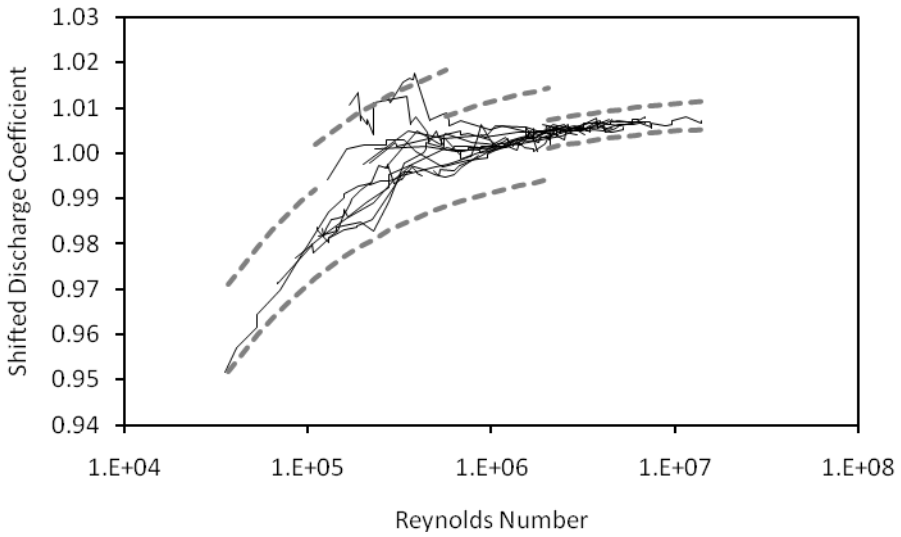

Figure 4: Calibrations Classified as Type A, Variable Statistical Interval

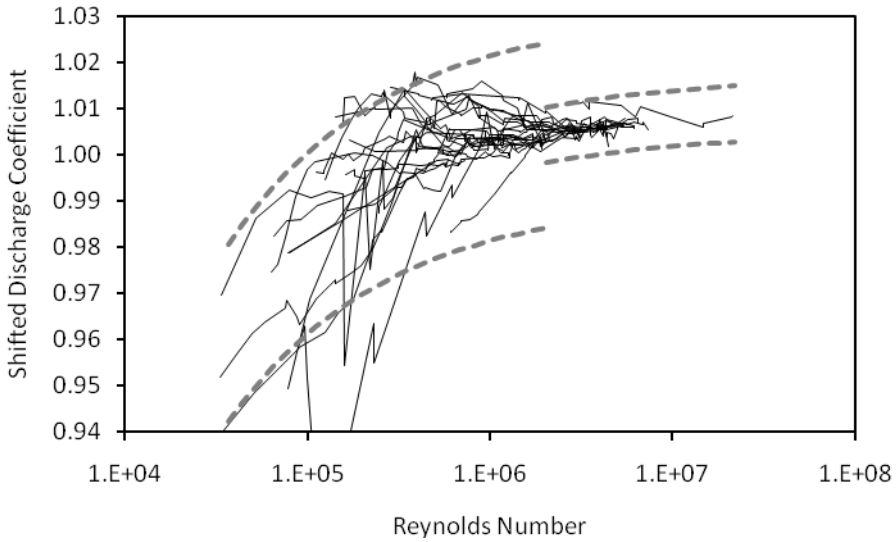

Figure 5: Calibrations Classified as Type B

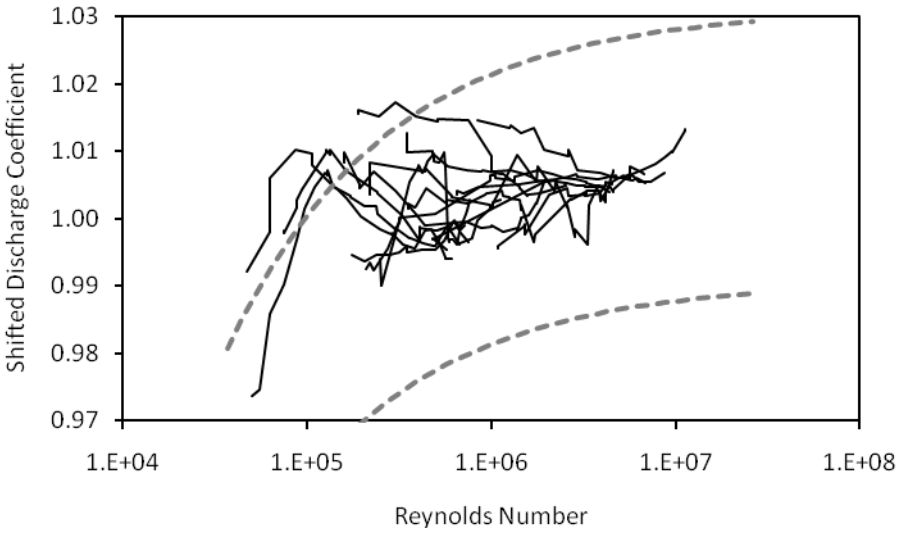

Figure 6: Calibrations Classified as Type C

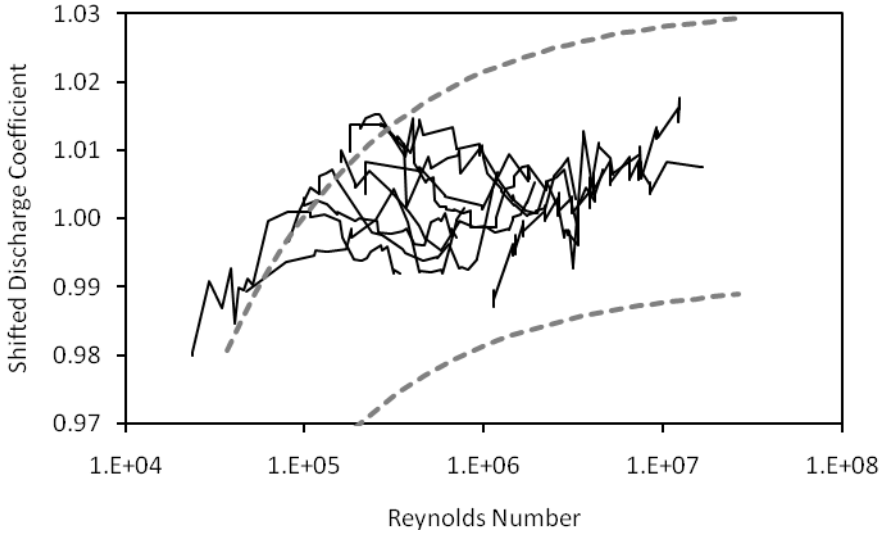

Figure 7: Calibrations Classified as Type D

Table 1: Summary of Test Parameters

	A	B	C	D
Calibrations [#]	20	28	14	14
Transition Hump [#]	9	22	10	9
Transition Hump [%]	45%	79%	71%	64%
Avg. C_d Shift	1.011	1.016	1.024	1.023
Min. C_d Shift	0.996	0.924	1.010	1.000
Max. C_d Shift	1.029	1.097	1.045	1.040
Rangeability	14.05	18.67	12.99	10.61
Avg. Hump Ampl. [%]	0.835	1.152	1.869	1.898
Avg. Inlet Dia. [cm]	10.177	9.697	13.879	18.77
Avg. Beta Ratio	0.544	0.502	0.508	0.535

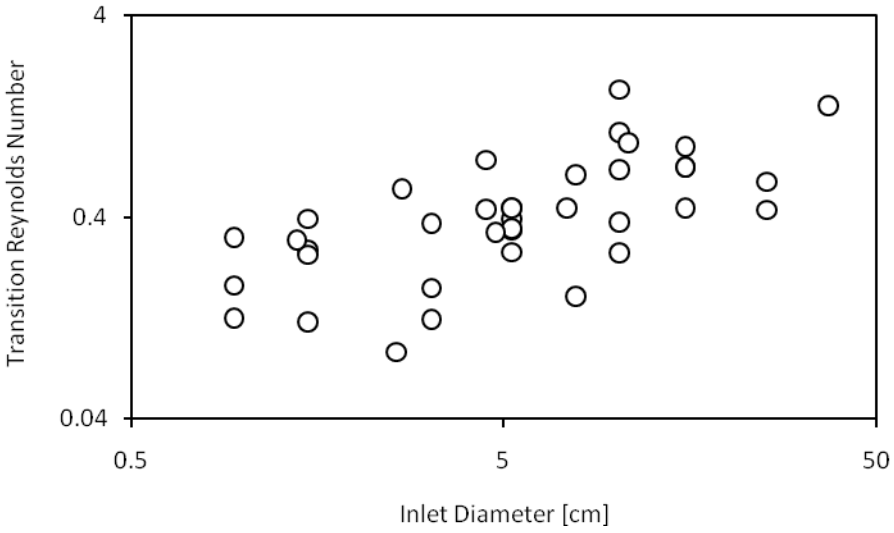

Figure 8: Boundary Layer Transition Reynolds Number as a Function of Venturi Inlet Diameter